



A comparative experimental evaluation of various Smith predictor approaches for a thermal process with large dead time



Carlos Mejía ^a, Estefanía Salazar ^a, Oscar Camacho ^{b,*}

^a Facultad de Ingeniería Eléctrica y Electrónica, Escuela Politécnica Nacional, Quito, Ecuador

^b Colegio de Ciencias e Ingenierías "El Politécnico", Universidad San Francisco de Quito USFQ, Quito 170157, Ecuador

Received 2 October 2021; revised 12 February 2022; accepted 18 March 2022

Available online 28 March 2022

KEYWORDS

Smith predictor;
Time-delay system;
Integral square error;
Two degrees of freedom scheme;
Practical application

Abstract This paper emphasizes a comparative experimental evaluation of three Smith predictor configurations. The three control schemes are tuned using different optimization algorithms; then, they are applied to an Arduino Temperature Control Lab used to test and evaluate their performance. The three deadtime compensators are compared using radial graphs. They were assessed under different conditions using various performance indices: the Integral Square Error, the Total Variations of Control Efforts, the Maximum Overshoot, and the Settling Time for tracking and disturbances changes. The Mejía et al. approach presented a better overall performance than the other two. Finally, the results showed that Smith Predictor is suitable for thermal processes with elevated dead time.

© 2022 THE AUTHORS. Published by Elsevier BV on behalf of Faculty of Engineering, Alexandria University. This is an open access article under the CC BY-NC-ND license (<http://creativecommons.org/licenses/by-nc-nd/4.0/>).

1. Introduction

There are numerous thermal systems in day-to-day industrial processes that require control. Some examples are heat exchangers, eco-friendly control in buildings, satellites, thermal packaging of electronic components, manufacturing, rapid thermal processing of computer chips, and others [27].

Typically, thermal systems include natural and forced convection, conduction, and radiation [14,1]. They are nonlinear and complex, containing complicated geometries, parameters variation with temperature, bifurcations, hydrodynamic instability, turbulence, and multiphase flow chemical reaction [17]. It is normal to have heat transfer coefficient values with errors due to utilizing lumped parameters as an option of distributed temperature fields or material characteristics that may not be exactly acknowledged. In consequence, generally, thermal systems are modeled using phenomenological concepts. Even when this is achievable, the dynamic model responses are challenging to define computationally in real-time [27]. On the other side, different factors produce some delay time to deliver energy efficiently [3,10]. One of the methods to compensate for

* Corresponding author.

E-mail addresses: carlos.mejia@epn.edu.ec (C. Mejía), estefania.salazar@epn.edu.ec (E. Salazar), ocamacho@usfq.edu.ec (O. Camacho).

Peer review under responsibility of Faculty of Engineering, Alexandria University.

dead time is Smith Predictor. It successfully takes the delay outside the control loop [4,12].

The interest in studying control strategies that compensate for time delays has grown in the last years. Korupu et al. [12] and Huba et al. [8] have presented reviews of the results of several papers dealing with approaches to the industrial control processes with time delay. Elevated dead time is commonly encountered besides thermal systems in other engineering systems such as chemical, biological, and teleoperation processes [7]. From the theoretical point of view, essential sources of delays can be physical and mathematical: the first ones due to transport of materials or fluids across long distances, measurement devices subject to lengthy processing, and final control elements that need some time to develop their activities, and the second ones due to order compensation in high order systems represented by low order models [3]. Hence, dead times cause late detection of disturbances and reduce the stability margins [4]. Moreover, by hand, they do not allow instantaneous reaction in the output variable when a variation in the manipulated variable occurs, but its effect only appears after the delay [20]. Thus, a high time delay increases the phase lag of the system considerably, impacting the stability of the closed-loop system [12].

The Smith Predictor (SP) was the first control scheme and one of the most industrially used to compensate for the time delays, and this is because it has a model of the process without delay in its structure [28]. However, the SP has presented some deficiencies associated with the accuracy of the model plant obtained. In practical applications, parameter uncertainties, internal/external disturbances, and delay variations cause a reduction of performance in the closed-loop control schemes. Therefore, several solutions have been suggested in the literature to deal with this problem, and some modifications to the original structure of the SP are done. Normey and Camacho [19] designed a filtered SP to improve the sensitivity to modeling errors; Zhang et al. [29] modified SP of two degrees of freedom (2DOF), increasing the system performance for reference changes and disturbances; Mejía et al. [16] modified SPs helping to compensate for measurable and non-measurable disturbances. Palmor & Powers [24], Huang et al. [9], Baez et al. [2] presented a robust SP improving performance in the face of uncertainties; Özbek and Eker [23] designed an optimal SP that help to improve the system response, among others.

Over the years, the development of various tuning methods increments delay compensation controllers, most of them based on first order plus dead time models. However, due to the limitations inherent in this method, good results were not always obtained [28]; thus, research about new alternatives, such as optimization algorithms, is an exploring area.

An optimization algorithm contains instructions that perform a task to solve a problem [11]. These algorithms use random search mechanisms based on the success of previous solutions to generate new solutions. The search mechanisms have a certain degree of diversity. For example, they can be found on a particular mapping function for the mutation (Mean-Variance Mapping Optimization) [6], on evolutionary methods used by living organisms (Genetic Algorithms) [5], or on the social behavior of insects, birds, and fish (Particles Swarm Optimization) [13].

The present work contains a comparative experimental evaluation of three deadtime compensators. The Smith predictor configurations considered are the Filtered Predictive Proportional Integral (FPPI) controller [18], the control scheme of two degrees of freedom of Zhang et al. [29], and the modified approach proposed by Mejía et al. [16]. The three control schemes are tuned using different optimization algorithms; then, they are applied to an Arduino Temperature Control Lab used to test and evaluate their performance. The three deadtime compensators are compared using radial graphs. Next, the experimental evaluation of the three control schemes was carried out. Then, they were evaluated under different conditions for tracking and disturbances changes using various performance indices such as the Integral Square Error, the Total Variations of Control Efforts, the Maximum Overshoot, and the Settling Time. The Mejía et al. approach presented a better overall performance than the other two. Finally, the results showed that Smith Predictor is suitable for thermal processes with elevated dead time.

The apports of this study can be summarized as follows:

- The Mejía et al. (2019) [16] approach was compared with two classical modified schemes obtaining excellent results. The Mejía et al. (2019) approach was used experimentally for the first time.
- The Mean-Variance Mapping Optimization (MVMO) algorithm, Genetic algorithms (GA), and Particles Swarm Optimization (PSO) were used to tune the three controllers to get the best tunning values for each scheme and make a fairer comparison. MVMO is the first time used for tuning the SP from the three optimization methods, resulting in the best global performance.
- The merits and drawbacks of each modified scheme were analyzed using radial graphs, comparing the control methods with different performance measures for set point and disturbances changes.

The organization of this work is as follows: Section 2 covers the basic concepts of the modified control strategies based on the SP, the optimization algorithms used to adjust the tuning parameters of the schemes under study, and the performance indices used to compare the results obtained. Section 3 presents the mathematical development of the proposed control scheme. Section 4 describes the physical process of temperature, its model identification, and the values of each control scheme's adjustment parameters when using the optimization algorithms. Section 5 shows the experimental results achieved for the temperature process with a dominant time delay, and finally, in Section 6 are the conclusions of this work.

2. Basic concepts

2.1. Control strategies

The modified control scheme uses the original Smith predictor and a First Order Plus Dead Time (FOPDT) model (1). This mathematical model allows us to compensate for time delays and describes the behavior of the system [21].

$$G_p(s) = \frac{K}{\tau s + 1} e^{-t_0 s} \quad (1)$$

2.1.1. Filtered Predictive Proportional Integral (FPPI) controller

Normey-Rico [18] modified the SP scheme, improving the system robustness when modeling errors occur, as shown in Fig. 1.

Where:

K system gain

τ system time constant

t_0 system time delay

The controller used is a classic PI that improves the dynamic response and reduces the steady-state error. The transfer function of a PI controller is described below:

$$\text{Controller}_{PI}(s) = K_p \left(1 + \frac{1}{K_i s} \right) \quad (2)$$

K_p and K_i are the proportional and the integral tuning parameters, respectively.

The filter considered in this control scheme is a first-order filter that also helps to reduce oscillations when modeling errors occur and can be represented as follows:

$$\text{Filter}(s) = \frac{1}{T_f s + 1} \quad (3)$$

Where the parameter T_f improves the robustness of the system, and the tuning is generally performed using Eq. (4).

$$T_f = \frac{t_0}{2} \quad (4)$$

2.1.2. Modified SP of W. Zhang et al.

Zhang et al. [29] changed the original structure of SPs and proposed a control scheme of two degrees of freedom (2DOF), decoupling the response of the system for reference changes and disturbances (see Fig. 2).

Where:

$r(s)$ reference

$y(s)$ process output

$u(s)$ control action

The first controller block is for reference changes, $G_r(s)$. Its structure depends on the invertible part of the plant model and the setting parameter λ_1 as follows:

$$G_r(s) = \frac{\tau s + 1}{K(\lambda_1 s + 1)} \quad (5)$$

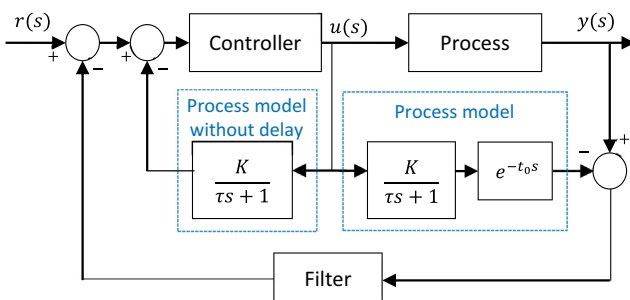


Fig. 1 FPPI scheme.

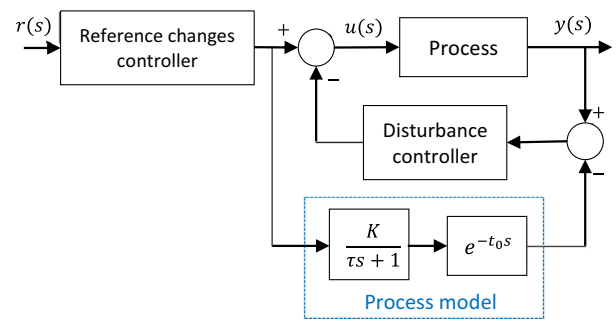


Fig. 2 Modified SP of W. Zhang et al.

The parameter λ_1 allows improving the response of the system for reference changes with $\lambda_1 > 0$ as a tuning condition. Fast responses are obtained when λ_1 approaches zero, but the robustness of the system decreases and vice versa.

A second controller block is for disturbance rejection. Its structure allows estimating disturbances, as shown in Fig. 3.

Where $M_0(s)$ represents a compensator of minimum order. It has the following structure:

$$M_0(s) = \frac{1}{K(\lambda_2 s + 1)} \quad (6)$$

The parameter λ_2 allows improving the rejection of disturbances with $\lambda_2 > 0$ as a tuning condition. Similar to the previous controller, faster compensation of the perturbations is obtained when the value of λ_2 approaches zero, but the robustness of the system decreases and vice versa.

2.2. Optimization algorithms

Optimization algorithms use random search mechanisms to have diversity and generate better solutions based on the success of the previous answers. In this work, the three optimization algorithms to find the most appropriate values of the adjustment parameters in the different control schemes are:

2.2.1. Mean-Variance Mapping Optimization (MVMO) algorithm

Mean-variance mapping optimization (MVMO) is an algorithm created and developed by Prof. István Erlich [10]. MVMO falls into the classification of the termed “population-based stochastic optimization techniques.” The basic concept reveals certain similarities with other heuristic methodologies. However, the new feature is a particular mapping function applied for mutating the descendants based on the mean and variance of the n-best population achieved so

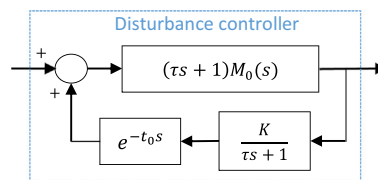


Fig. 3 Structure of the disturbance controller of the Zhang scheme.

far. Furthermore, the internal search range of all variables is restricted to $[0,1]$.

Nevertheless, the function evaluation is always conducted in the original scales. The critical feature of MVMO is a particular mapping function described by the mean and shape variables, considering the mean and variance of the best solutions achieved so far. Thus, this algorithm operates with a unique solution instead of a group of keys to perform a fast and accurate optimization with a minimum of objective function evaluations [6]. Fig. 4 illustrates the flow diagram of the MVMO algorithm.

2.2.2. Genetic Algorithms (GA)

GA are evolutionary methods based on living organisms and can solve search and optimization problems. The GA works with a population of individuals, representing a solution. Each individual is assigned a value that relates to the goodness of that solution [11]. The higher the performance of an individual to the problem, the higher the probability that it is selected to cross his genes with another individual, thus generating a new population with possible better solutions, which replace the previous one [5]. Fig. 5 shows the flow diagram of this algorithm.

2.2.3. Particles Swarm Optimization (PSO)

PSO is an optimization technique centered on the social behavior of insects, birds, and fish. In PSO, this behavior is represented by particles part of a population and have a particular position and speed in a search space. The initial population is determined randomly, and each particle moves through the search space to find the best position. Then, each

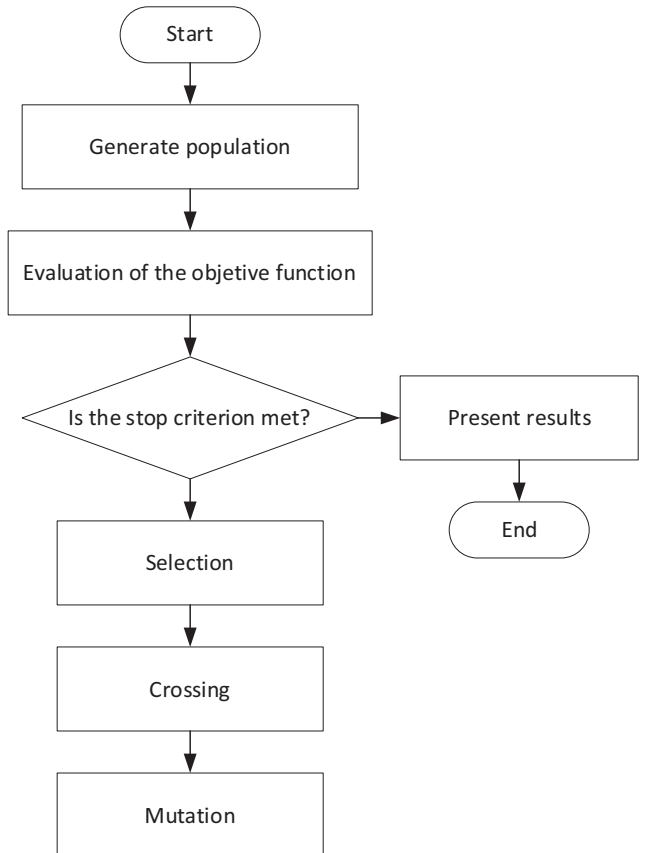


Fig. 5 Flow diagram of Genetic Algorithms.

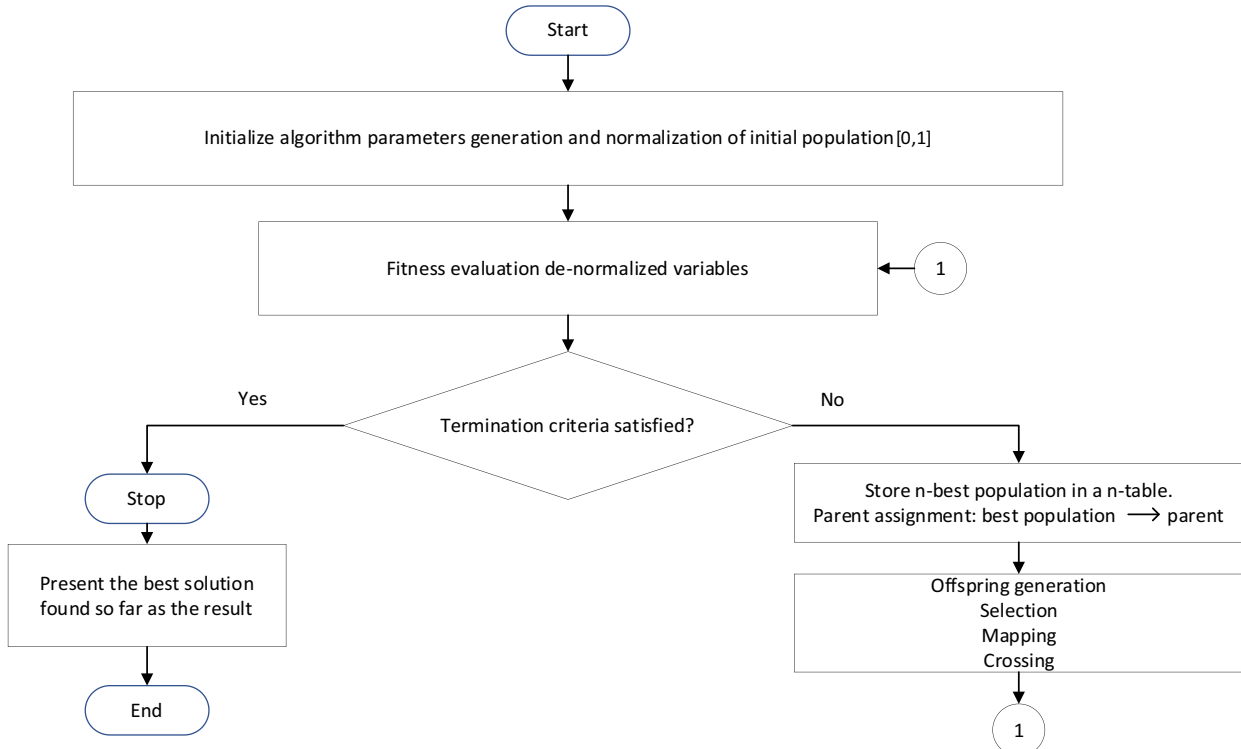


Fig. 4 Flow diagram of the MVMO algorithm.

particle communicates the best position to the other particles, and in this way, the particles tend to move to a better search space to minimize the objective function [13]. The flow diagram of the PSO algorithm, Fig. 6, is:

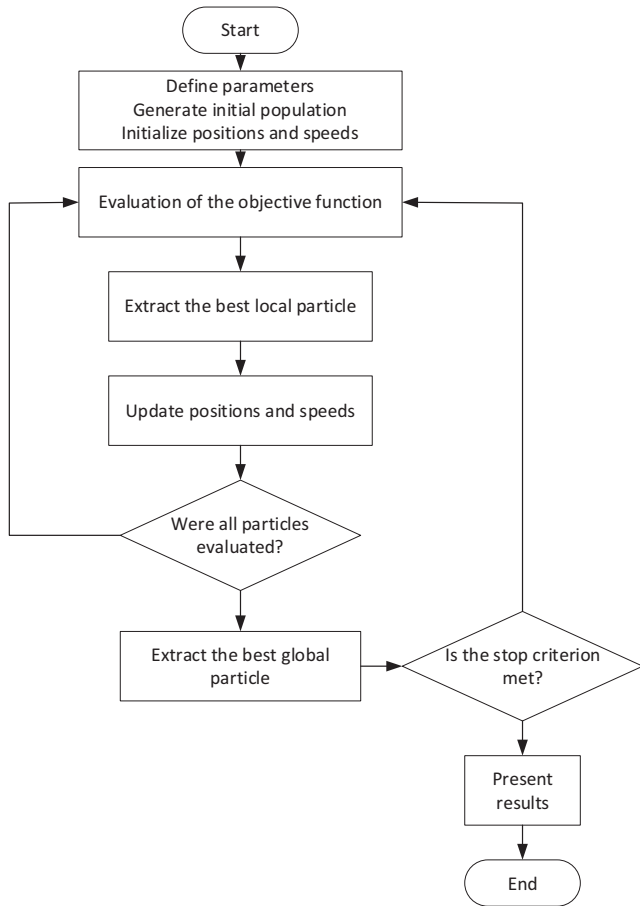


Fig. 6 Flow diagram of the PSO algorithm.

2.3. Performance indices

Performance indices [28,15] are used to indicate and compare the performance of each control scheme. The performance indices used in this document are the Integral Square Error (ISE), The Total Variations of Control Efforts (TVu), the Maximum Over Impulse in percentage (%Mp), and the settling Time (Ts).

3. Smith predictor proposal design

In Fig. 7, some modifications are made to the original structure of the SP to obtain the proposal. First, the new approach introduces a first-order filter to decrease oscillations of modeling errors. Secondly, the response to reference changes and disturbances became independent through a scheme of two degrees of freedom. Finally, feedback of the estimated disturbances is added to the model without delay to compensate for the disturbances quickly.

Where:

$G_r(s)$: Controller for reference changes

$G_d(s)$: Controller for disturbances

$D(s)$: Transfer function for disturbance estimation

$M(s)$: First-order filter

The procedure to determine the transfer function between output $y(s)$ and reference $r(s)$, Fig. 7 considers that the disturbance $d(s) = 0$.

From the control structure, Fig. 7, Eqs. (7), (8), (9), and (10) are:

$$\begin{aligned} e(s) &= r(s)G_r(s) - M(s)[y(s) - y_e(s)] \\ &\quad - G_n(s)[u(s) + D(s)(y(s) - y_e(s))] \end{aligned} \quad (7)$$

$$u(s) = e(s)G_d(s) \quad (8)$$

$$y(s) = u(s)G_p(s) \quad (9)$$

$$y_e(s) = u(s)G_n(s)e^{-t_0 s} \quad (10)$$

Substituting (9) into (10):

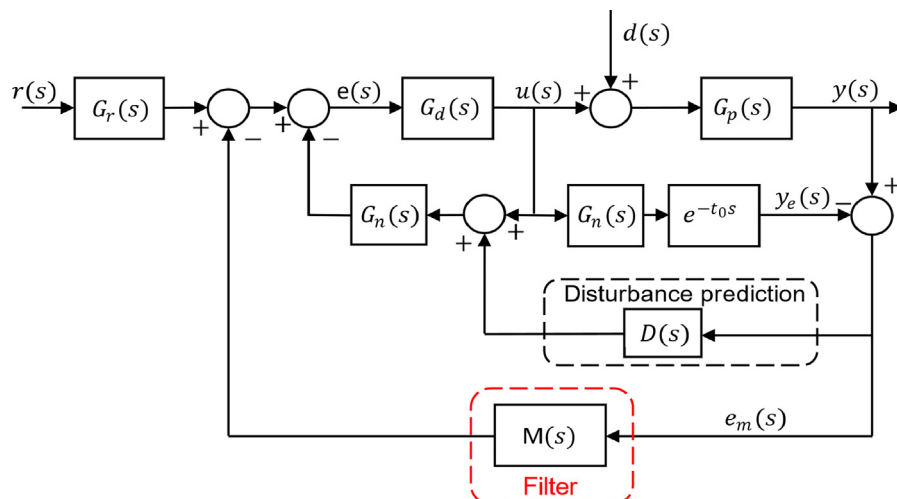


Fig. 7 Block diagram of the New Proposal of the Smith Predictor.

$$y_e(s) = \frac{y(s)G_n(s)e^{-t_0s}}{G_p(s)} \quad (11)$$

Assuming that the modeling error is zero ($e_m = 0$), we can say:

$$G_p(s) = G_n(s)e^{-t_0s} \quad (12)$$

Replacing (12) into (11):

$$y_e(s) = y(s) \quad (13)$$

From (13), the equation (7) is now:

$$e(s) = r(s)G_r(s) - G_n(s)u(s) \quad (14)$$

Substituting (8) and (9) into (14), results:

$$y(s) = r(s)G_r(s)G_d(s)G_p(s) - y(s)G_n(s)G_d(s) \quad (15)$$

Finally, rearranging (15) is obtained:

$$\frac{y(s)}{r(s)} = \frac{G_r(s)G_d(s)G_p(s)}{1 + G_n(s)G_d(s)} \quad (16)$$

The denominator of (16) does not present time delay; however, the output when reference changes are made on the parameters of $G_r(s)$ and $G_d(s)$.

Now the transfer function between output $y(s)$ and disturbance $d(s)$ of the scheme of Fig. 7 is determined. It considered that the disturbance $d(s) \neq 0$. This relation is determined from Eqs. (17), (18), (19), and (20).

$$\begin{aligned} e(s) &= -M(s)[y(s) - y_e(s)] \\ &\quad - G_n(s)[u(s) + D(s)(y(s) - y_e(s))] \end{aligned} \quad (17)$$

$$u(s) = e(s)G_d(s) \quad (18)$$

$$y(s) = G_p(s)[u(s) + d(s)] \quad (19)$$

$$y_e(s) = u(s)G_n(s)e^{-t_0s} \quad (20)$$

Substituting (19) into (20), it results:

$$y_e(s) = \frac{[y(s) - d(s)G_p(s)]G_n(s)e^{-t_0s}}{G_p(s)} \quad (21)$$

Assuming that the modeling error is zero ($e_m = 0$), we can say:

$$G_p(s) = G_n(s)e^{-t_0s} \quad (22)$$

Replacing (22) into (21):

$$y_e(s) = y(s) - d(s)G_p(s) \quad (23)$$

Substituting (18) and (23) into (17) and simplifying, is obtained:

$$\begin{aligned} \frac{u(s)}{G_d(s)} &= -M(s)[d(s)G_p(s)] \\ &\quad - G_n(s)[u(s) + D(s)(d(s)G_p(s))] \end{aligned} \quad (24)$$

Replacing (19) into (24), it results:

$$\begin{aligned} y(s) - d(s)G_p(s) &= -d(s)M(s)G_p(s)G_d(s)G_p(s) \\ &\quad - y(s)G_n(s)G_d(s) + d(s)G_n(s)G_d(s)G_p(s) \\ &\quad - d(s)D(s)G_p(s)G_n(s)G_d(s)G_p(s) \end{aligned} \quad (25)$$

Finally, rearranging (25) is obtained:

$$\frac{y(s)}{d(s)} = G_p(s) \left[1 - \frac{M(s)G_p(s)G_d(s) + D(s)G_p(s)G_n(s)G_d(s)}{1 + G_n(s)G_d(s)} \right] \quad (26)$$

In Eq. (26), it can be seen that the output of the system when disturbances occur depends on the parameters of $G_d(s)$, $M(s)$, and $D(s)$.

From the transfer functions (16) and (26), the parameters of $M(s)$ and $D(s)$ affect the response of the system only when disturbances occur; however, the parameters of $G_d(s)$ affect the output when reference changes and disturbances occur. To have a scheme of two degrees of freedom (2DOF) and that the responses of the system are independent, considerations (27) and (28) are necessary. The structure of $G_d(s)$ is similar to a classical PI. To have a scheme of 2DOF, the proportional and integral constant of $G_d(s)$ are determined from the approximate model without delay ($G_n(s)$). On the other hand, $G_r(s)$ is a filter to improve the response of the process for reference changes. The responses of the system are independent of the structure of $G_r(s)$ as indicated in (28), where τ is the time constant of the approximate model without delay ($G_n(s)$) and λ_1 is an adjustment parameter.

$$G_d(s) = \frac{1}{K} \left(1 + \frac{1}{\tau s} \right) \quad (27)$$

$$G_r(s) = \frac{\tau s + 1}{\lambda_1 s + 1} \quad (28)$$

Replacing (27) and (28) in (16) it is obtained the transfer function between output $y(s)$ and reference $r(s)$.

$$\frac{y(s)}{r(s)} = \frac{e^{-t_0s}}{\lambda_1 s + 1} \quad (29)$$

Similarly, replacing (27) and (28) in (26) it is obtained the transfer function between output $y(s)$ and disturbance $d(s)$.

$$\frac{y(s)}{d(s)} = G_p(s) \left[1 - \frac{M(s)e^{-t_0s} + D(s)G_p(s)}{\tau s + 1} \right] \quad (30)$$

Now, observing the transfer functions (29) and (30), it can be said that the responses of the system for reference changes and disturbances are independent. For the one case, it only depends on the λ_1 parameter, and for the other case, it depends on the adjustment parameters of $M(s)$ and $D(s)$.

The $M(s)$ filter allows improving the robustness or performance of the system when disturbances or modeling errors occur through the adjustment parameter λ_2 as indicated in Eq. (31). This parameter must meet the following condition $\lambda_2 > 0$. If the value of λ_2 is near to zero, system performance increases, but the robustness decreases. On the other hand, if the value of λ_2 is far from zero, system performance decreases, but the robustness increases.

$$M(s) = \frac{1}{\lambda_2 s + 1} \quad (31)$$

To quickly compensate for the disturbances that may occur in the process, the estimated disturbances obtained by $D(s)$, are feedback to the approximate model without delay ($G_n(s)$) Fig. 7). The structure of $D(s)$ is presented in (32), which has an adjustment parameter and must be greater than zero ($\lambda_3 > 0$). If the value of λ_3 is near to zero, the disturbances can be compensated quickly. On the other hand, if the value of λ_3 is far from zero, the time to compensate for the distur-

bances increases. In the case of two or more disturbances with different effect times on the process output, the proposed scheme (Fig. 7) compensates them. However, $D(s)$ has the same effect on all disturbances occurring in the process; for this reason, it is recommended that the parameter λ_3 should be adjusted considering the disturbance that has the most significant amplitude.

$$D(s) = \frac{K}{\lambda_3} s \quad (32)$$

4. Thermal process with time delay

4.1. Temperature control laboratory overview

The Temperature Control Laboratory (TCLab) application of feedback control comprises an Arduino Leonardo, a LED, two heaters, and two temperature sensors, as shown in Fig. 8 [22]. In Park et al. [25], several applications for this module can be found.

The control objective in this process is to keep the temperature at the desired value by manipulating the output power of the heater (by varying the pulse width of the PWM, Pulse Width Modulation) [26]. Heater one (SISO system) was used to test the delay compensation schemes, and heater two was used to perform disturbances on the environmental temperature of the process (initial temperature condition), besides a software time delay of 230 [s] was added to the sensor output.

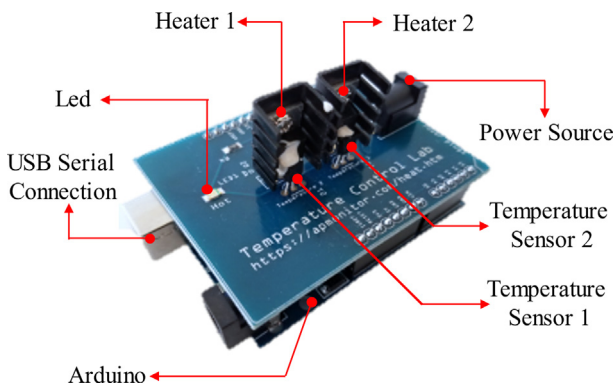


Fig. 8 Temperature control laboratory.

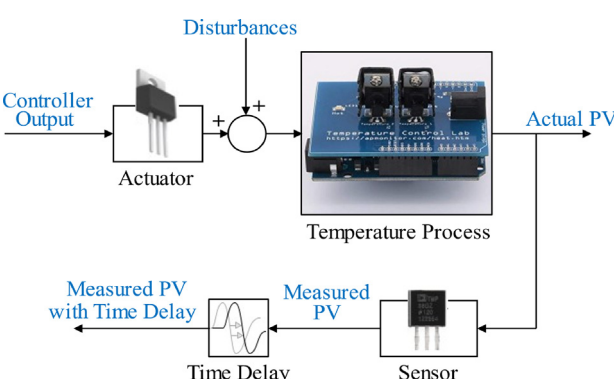


Fig. 9 Temperature process block diagram.

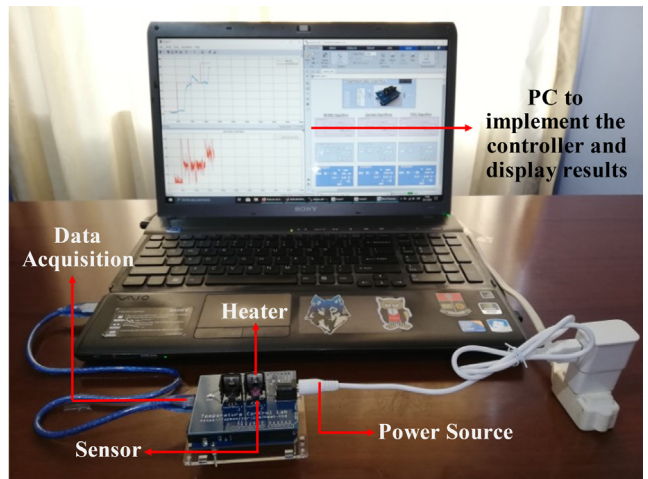


Fig. 10 Temperature control laboratory.

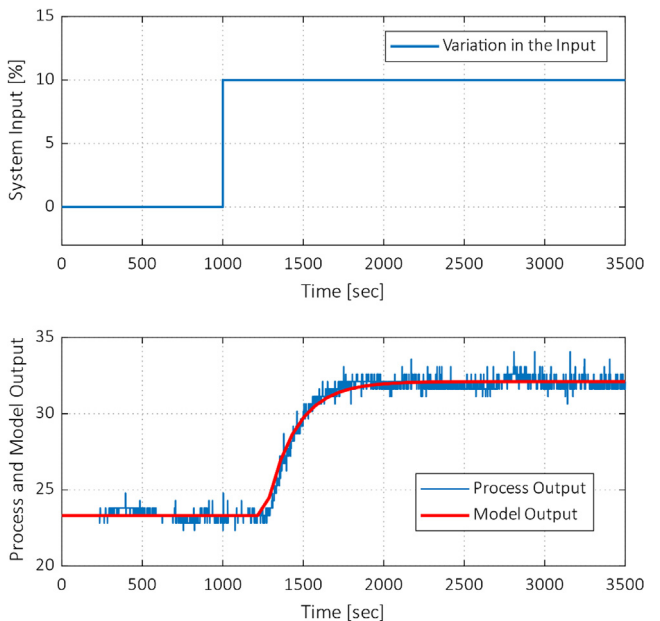


Fig. 11 Process and Model Output validation.

Table 1 Parameters of optimization algorithms.

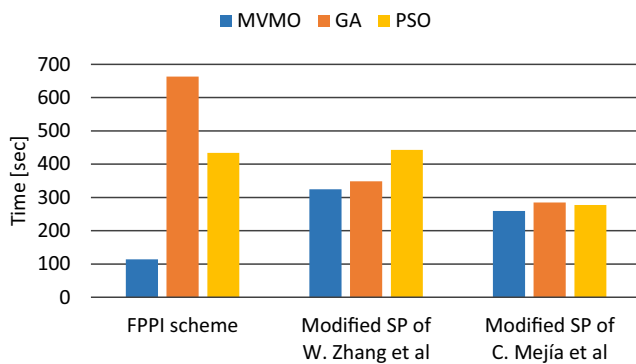
	MVMO	GA	PSO
Number of generations	200	50	50
Size of the population	1	20	20
Total iterations	200	1000	1000

The scheme of Fig. 9 shows the place where this time delay was added and the process variable that is fed back to perform the temperature control.

Fig. 10 illustrates the connection control system for this process. Where it can be seen that the TCLab system is connected to a PC through the Arduino board that allows data

Table 2 Parameters of the three-time delay compensation schemes.

Algorithm	Parameters of the FPPI controller			Parameters of the 2DOF of W. Zhang et al. scheme		Parameters of the 2DOF of C. Mejía et al. scheme		
	K_p	K_i	T_f	λ_1	λ_2	λ_1	λ_2	λ_3
MVMO	9.5310	0.0081	1.3793	21.9360	14.7784	19.7394	15.0421	0.1710
GA	10.5738	0.0144	0.1567	24.1726	17.5821	21.8704	31.4644	0.1340
PSO	9.1387	0.0154	0.1379	21.7312	14.8122	21.8465	15.4646	0.2546

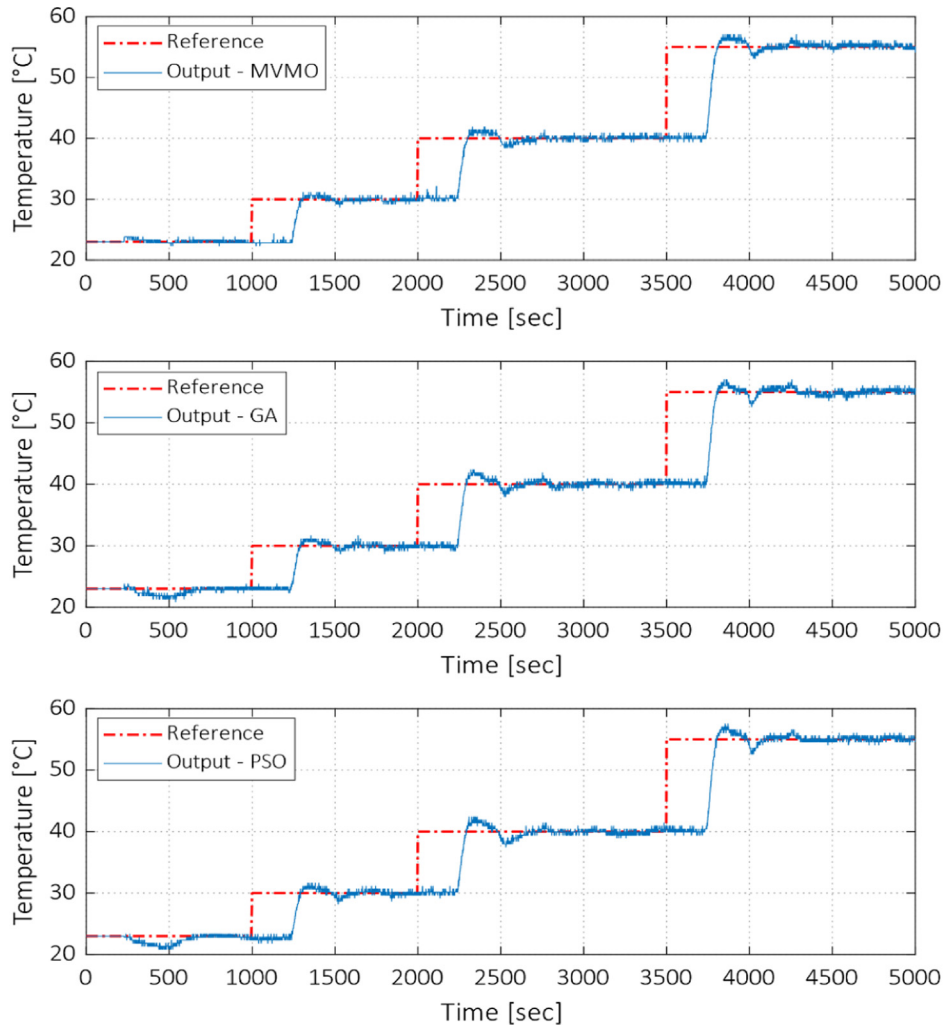
**Fig. 12** Comparison of convergence times.

acquisition, and with the help of the Matlab Real-Time Toolbox, different control techniques are developed in real-time.

4.2. Process model identification

The TCLab process can be approximated to a reduced-order model. The FOPDT model is obtained from the reaction curve method. A step change of 10% in the input of the system is done [21], resulting in (33). Fig. 11 shows the model and process outputs after applying the reaction curve method.

$$G(s) = \frac{0.8801}{182.25s + 1} e^{-258.692s} \quad (33)$$

**Fig. 13** Output process using the FPPI scheme.

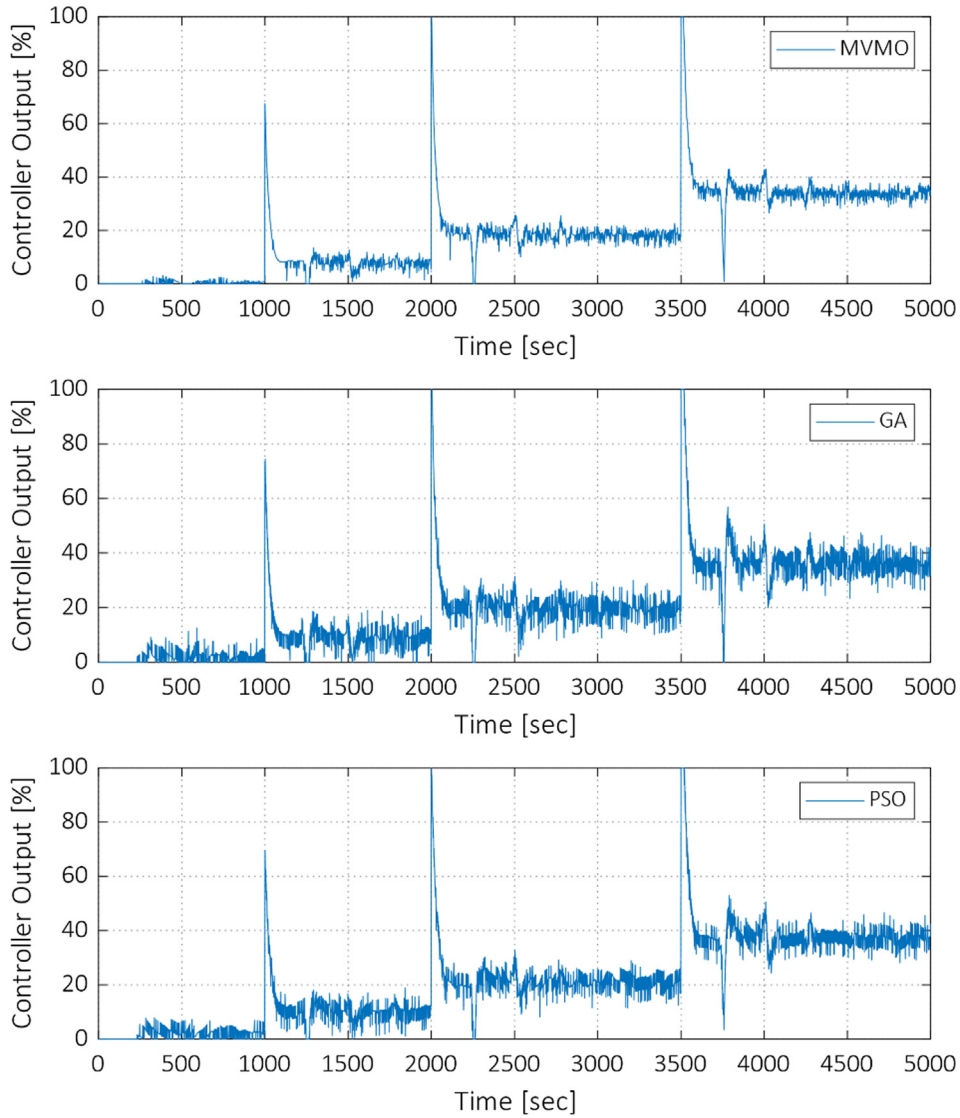


Fig. 14 Control output signal using the FPPI scheme.

4.3. Tuning parameters from optimization algorithms

This section presents the parameter values of each control scheme tuned by MVMO, GA, and PSO. The difference between the three optimization algorithms is the mechanism used to generate new populations and the total number of iterations, as shown in [Table 1](#).

The values of the adjustment parameters of the FPPI, W. Zhang, and C. Mejía schemes are found in [Table 2](#); these values were obtained using the description of the three optimization algorithms of Section 2.2 and considering the ISE performance index. Also, equations described in Section 2.1 were used to adjust the parameters of each scheme.

[Fig. 12](#) shows a graphical comparison of convergence times of the optimization algorithms for each of the control schemes, where it is seen that MVMO converged in less time than the

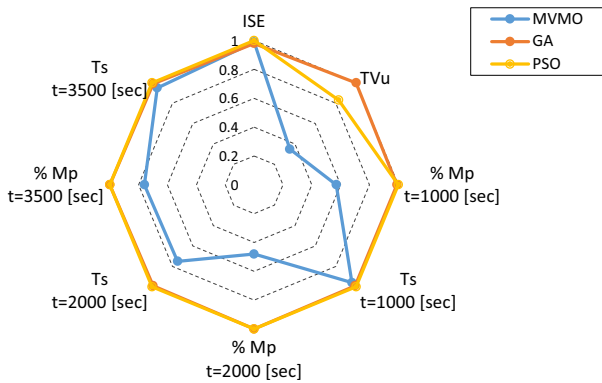


Fig. 15 Performance indices comparison for the FPPI scheme.

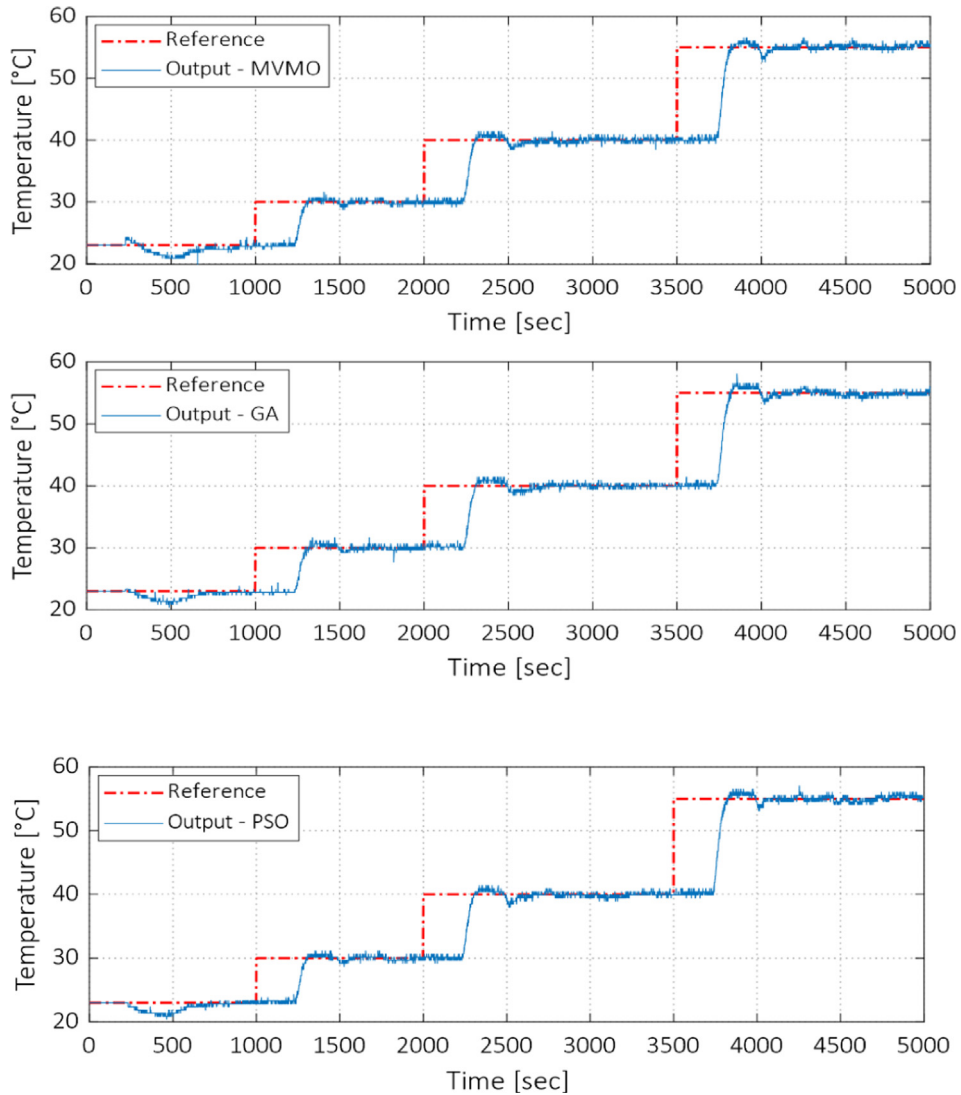


Fig. 16 Output process using the 2DOF scheme of W. Zhang.

other two algorithms. The total iterations of the MVMO algorithm are five times less than the different algorithms, as seen in Table 1. Therefore, from the point of view of convergence time, MVMO results in the best optimization algorithm.

5. Experimental results

The three delay schemes were proved once the reduced-order model for the TCLAb was obtained and the optimization algorithms tested. Thus, the experimental results for setpoint and disturbances changes are presented in this section.

5.1. Setpoint changes experiments.

The controllers are adjusted to MVMO, GA, and PSO algorithms. First, the initial process temperature set to 23 °C was

varied to 30 °C, then this value was changed to 40 °C and finally to 55 °C. Each control scheme is tested individually firstly, and in the last part of the section, a comparison among the three is made using different performance indices.

5.1.1. Modified SP of Normey-Rico (FPPI)

Fig. 13 shows the system output for reference changes. The graph is divided into three parts, considering the three tuning optimization algorithms. The response of the system changes depending on the optimization algorithm used to adjust the parameters. For example, when the control scheme FPPI is adjusted to the MVMO optimization algorithm, it presents a smoother response than the system response when it is adjusted to the GA and PSO algorithms (Fig. 13).

Additionally, it can be seen in Fig. 14 that the control scheme FPPI adjusted by the MVMO algorithm had smoother

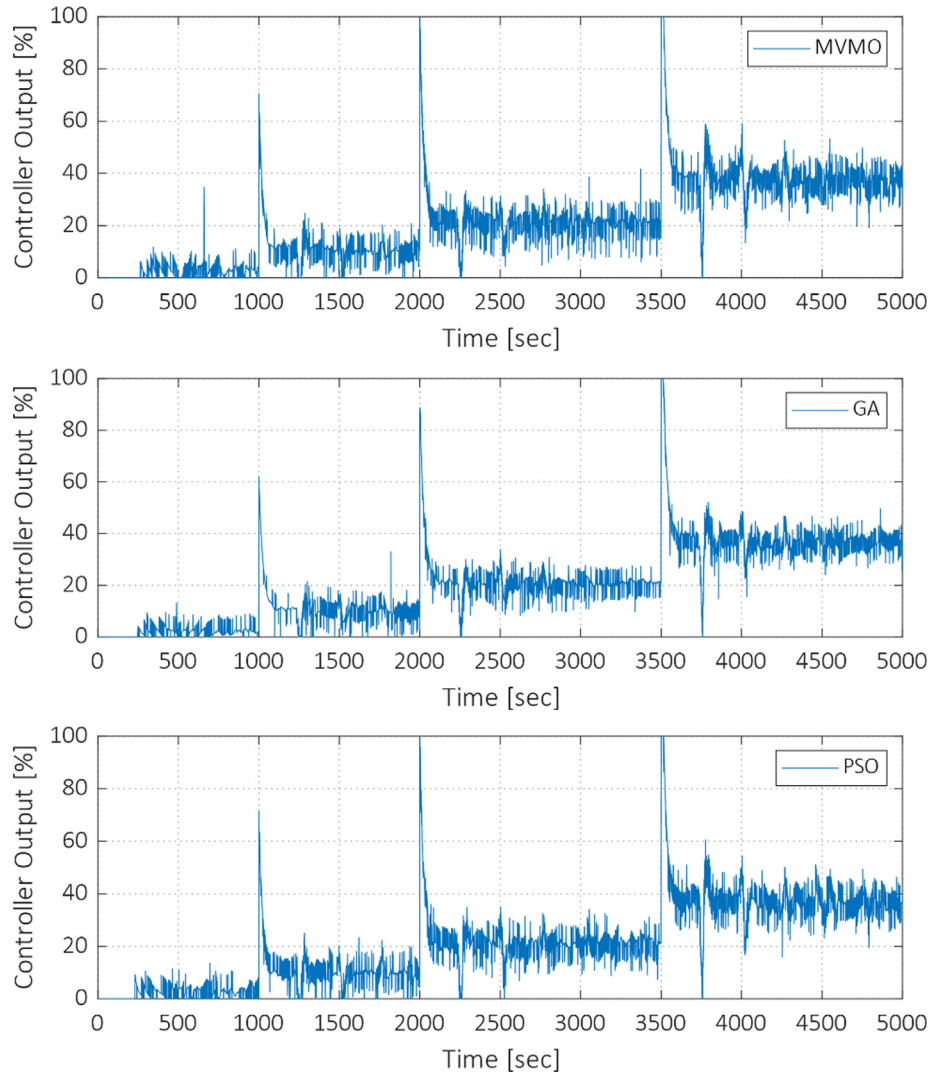


Fig. 17 Control signal using the 2DOF scheme of W. Zhang.

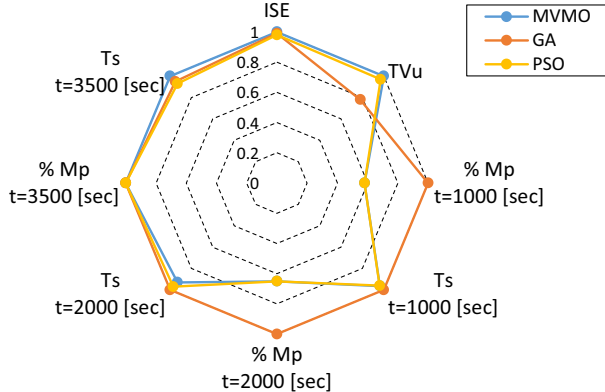


Fig. 18 Performance indices comparison for the 2DOF scheme of W. Zhang et al.

control signals (the lowest control effort) when reference changes were done. Therefore, it can help with the lifetime of the valve.

Radial Graphs are multi-axis graphs that display similar ideas in one graphical presentation; thus, a radial graph is made (Fig. 15) to show all performance indices in one plot. The radial graph was normalized, considering one as the worst case. The idea is to visualize and know which optimization algorithm can present more advantages when adjusting the FPPI scheme parameters. Fig. 15 shows that the FPPI scheme adjusted by the MVMO optimization algorithm has the lowest values in the TVu, Mp, and Ts indices when reference changes are made. Therefore, the optimization algorithm that presents the smallest area in the radial graph can perform better. Hence, the FPPI control scheme adjusted by the MVMO algorithm is better than the other two algorithms when reference changes occur.

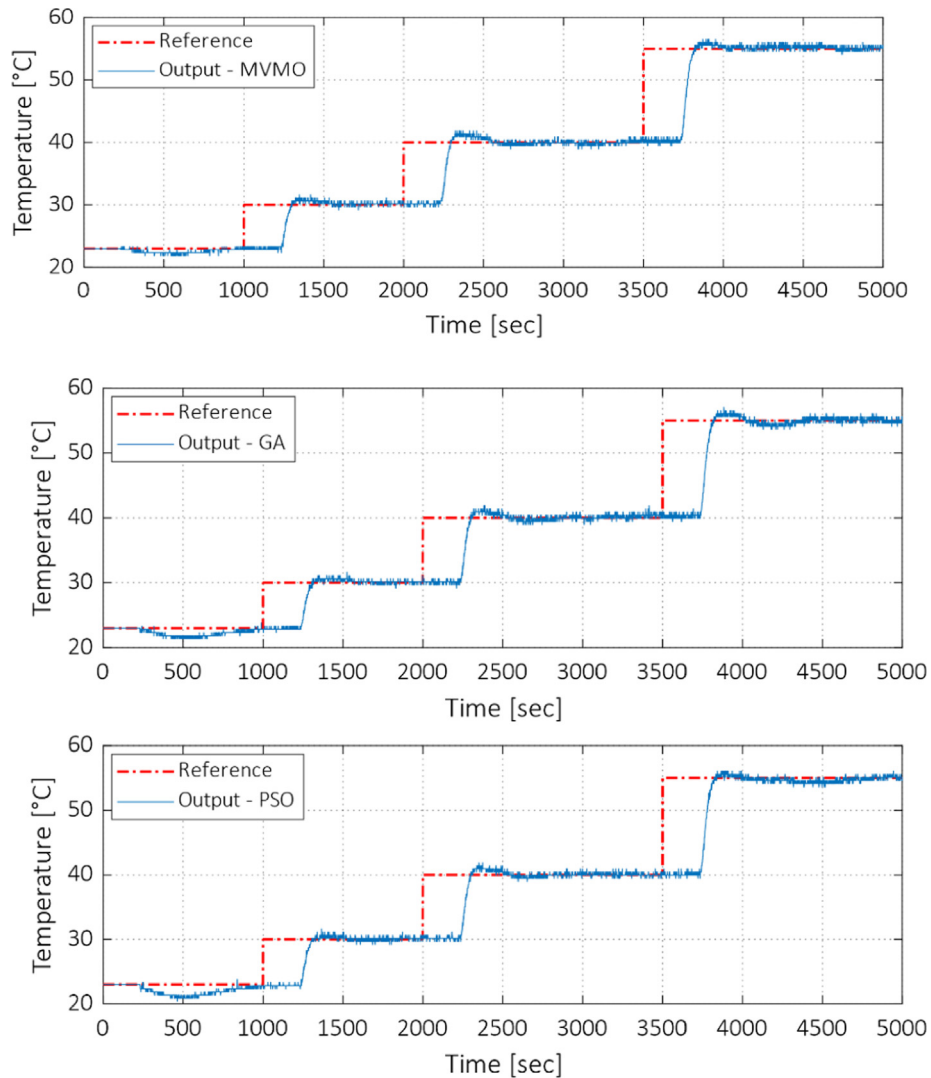


Fig. 19 Output process using the 2DOF scheme of C. Mejía et al.

5.1.2. Modified SP of 2DOF of W. Zhang et al

In this subsection, a similar procedure as above is presented. Fig. 16 shows that the response of the system for reference changes is very close for the three tuning methods (MVMO, GA, and PSO) when using the 2DOF scheme of W. Zhang.

Additionally, in Fig. 17, the control actions for each tuning are presented, where it can be seen that the 2DOF scheme of W. Zhang tuned by GA offers a smoother control action than the adjustment by MVMO and PSO.

In the radial graph of Fig. 18, it can be seen that the W. Zhang's 2DOF control scheme adjusted by PSO has lower values of the performance indices (ISE; Mp and Ts for $t = 1000$ [s]; Mp for $t = 2000$ [s]; Mp and Ts for $t = 3500$ [s]). On the other hand, when the parameters are adjusted with GA, it has

the smallest value in the TVu index (smooth control actions). When MVMO makes changes in the W. Zhang 2DOF control scheme, it presents the Mp with the lowest and identical values of PSO. In summary, in the radial graph depicted in Fig. 18, it can be seen that W. Zhang's 2DOF control scheme adjusted by PSO has better global performance since it presents a smaller area than that of the other two algorithms.

5.1.3. Modified SP of 2DOF of C. Mejía et al

Similar to the previous two cases, the procedure is applied to the Mejía et al. control approach. Fig. 19 shows the system response for reference changes when the 2DOF scheme of C. Mejía is tuned by different optimization algorithms (MVMO, GA, and PSO). For example, when the temperature is changed

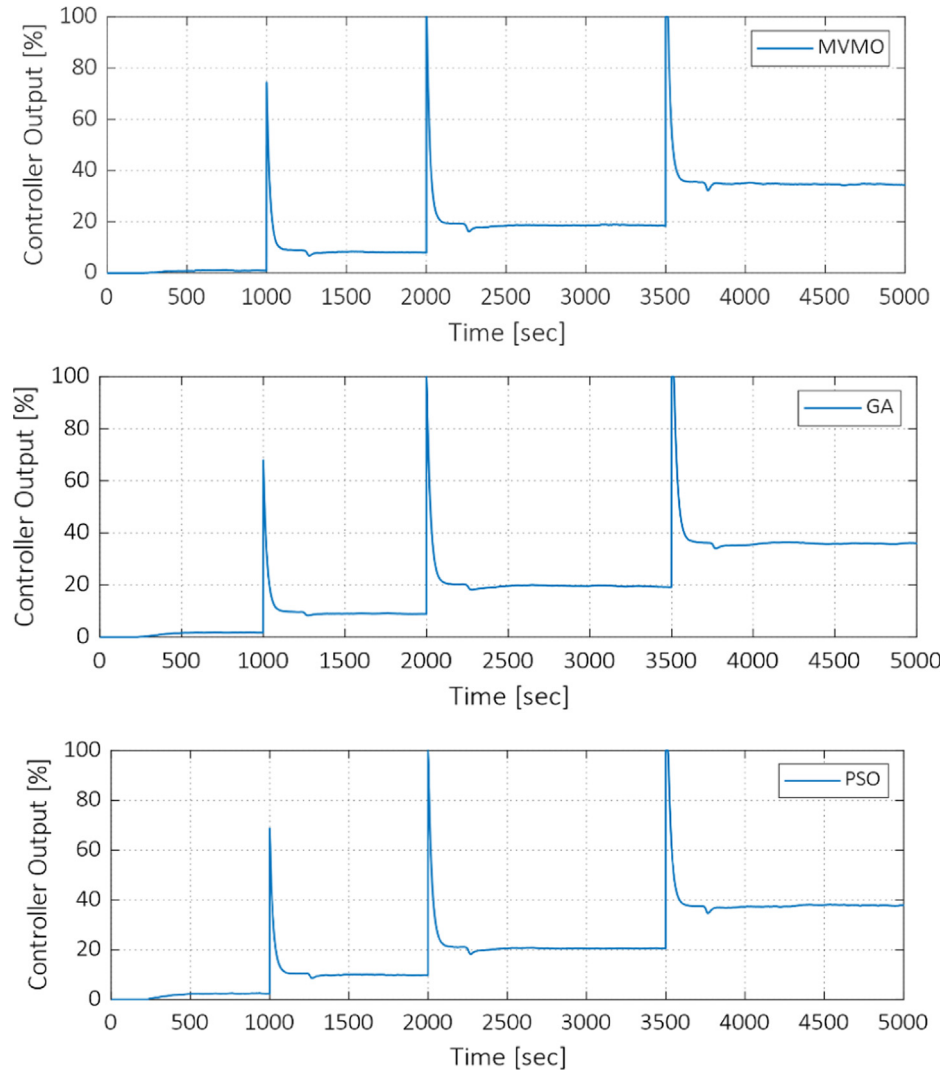


Fig. 20 Control signal using the 2DOF scheme of C. Mejia et al.

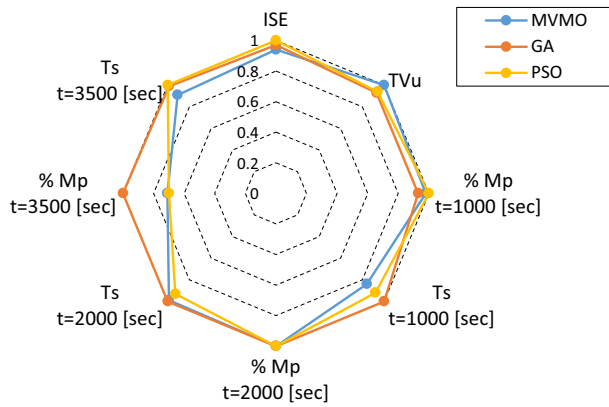


Fig. 21 Performance indices comparison for the 2DOF scheme of C. Mejia et al.

from 40 °C to 55 °C, it can be seen that the scheme tuned by MVMO stabilizes faster than the system response when GA and PSO adjust the parameters.

Fig. 20 shows the control signals of the 2DOF scheme of C. Mejia for each of the tunings, where it can be seen that the system tuned by GA has a smoother control action than the other two algorithms (MVMO and PSO).

The radial graph of **Fig. 21** compares the performance indices of the 2DOF scheme of C. Mejia for each tuning algorithm. It can be seen that the 2DOF of C. Mejia adjusted by MVMO has four lower values of the performance indices (ISE; Ts for $t = 1000$ [s]; Mp for $t = 2000$ [s] and Ts for $t = 3500$ [s]). On the other hand, when the parameters are adjusted with GA, it has the smallest value in the TVu index (soft control actions). Furthermore, when PSO changes the 2DOF of C. Mejia, it has the lowest Mp in $t = 3500$ [s]. However, in the radial graph in **Fig. 21**, it can be seen that the 2DOF control scheme of C. Mejia, adjusted by MVMO, has

a little better performance for reference changes because it presents a smaller area of the other two algorithms.

5.2. Comparison of the three delay compensation control schemes

In this part, the FPPI, 2DOF of W. Zhang et al., and 2DOF of C. Mejía et al. schemes are compared using the best results associated with the optimization algorithm that presented the best global performance for each scheme case as shown above. Fig. 22 shows that the 2DOF scheme of C. Mejía tuned by MVMO has a smoother response and stabilizes more quickly than the response given by the other two control schemes when changes occur in the process temperature.

The control signals of the three delay compensation schemes are illustrated in Fig. 23; It is shown that the 2DOF scheme of C. Mejía has the control signal without noise in comparison to the control signals of the other two schemes because this control scheme has a filter that attenuates the noise in the signal. On the other hand, the FPPI and 2DOF schemes of W. Zhang have noise in the control signal. However, the FPPI scheme has less noise than the 2DOF scheme

of W. Zhang because this scheme has a first-order filter in its structure.

In the radial graph of Fig. 24, a comparison of different performance indices for the three control schemes is exposed. The radial graph of Fig. 24 shows that the 2DOF control scheme of C. Mejía et al., tuned by MVMO, presents better global performance than the FPPI schemes tuned by MVMO and the 2DOF scheme of W. Zhang et al. optimized by PSO. Furthermore, the 2DOF system of C. Mejía et al. has the smallest area in the radial graph.

5.3. Experimental tests for disturbances

Once, several tests for tracking were made, disturbance tests were carried out in the process. The temperature in heater two was varied, indirectly producing a temperature increase in heater one. Two disturbances are made when the process is at 40 [°C]; the first disturbance is performed at 3000 [s], making a 40% increase in the input of heater two, and the second disturbance is achieved at 6000 [s], producing a 40% decrease in the input of heater two. Fig. 25 shows the results obtained when performing the disturbances in the temperature process.

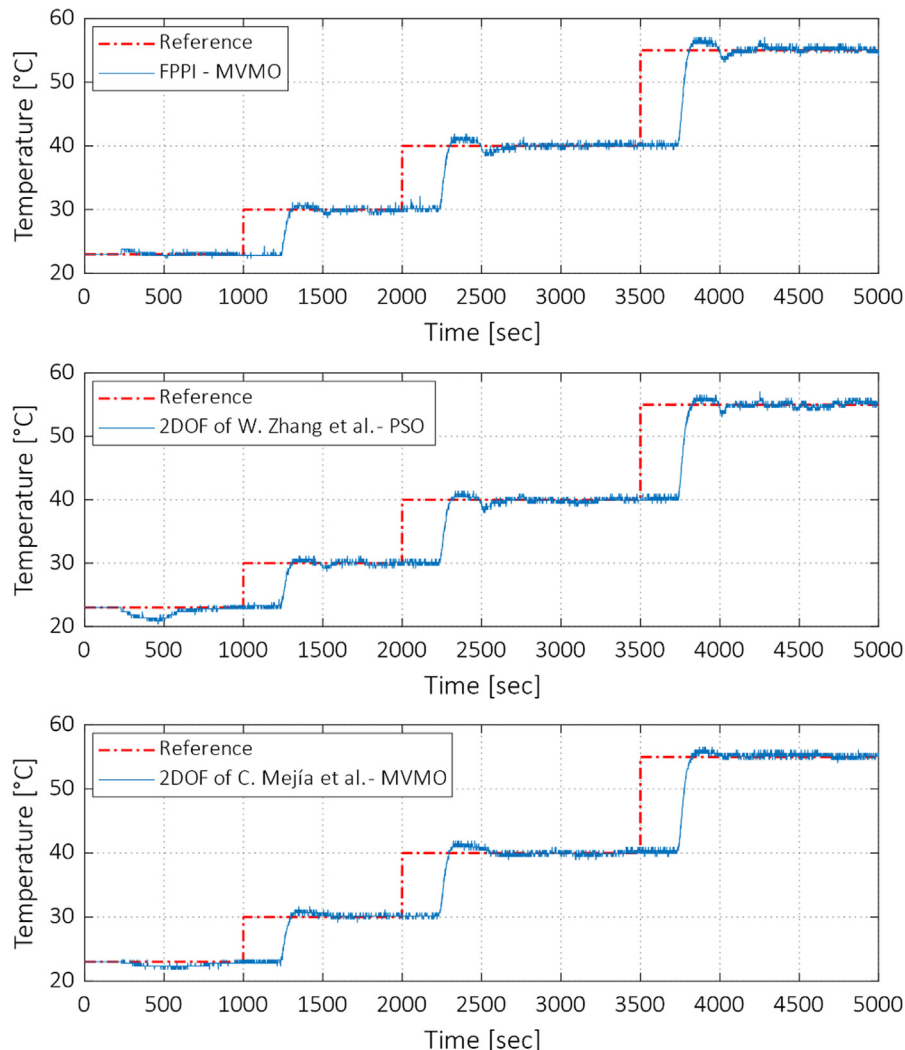


Fig. 22 Output process for the three control schemes.

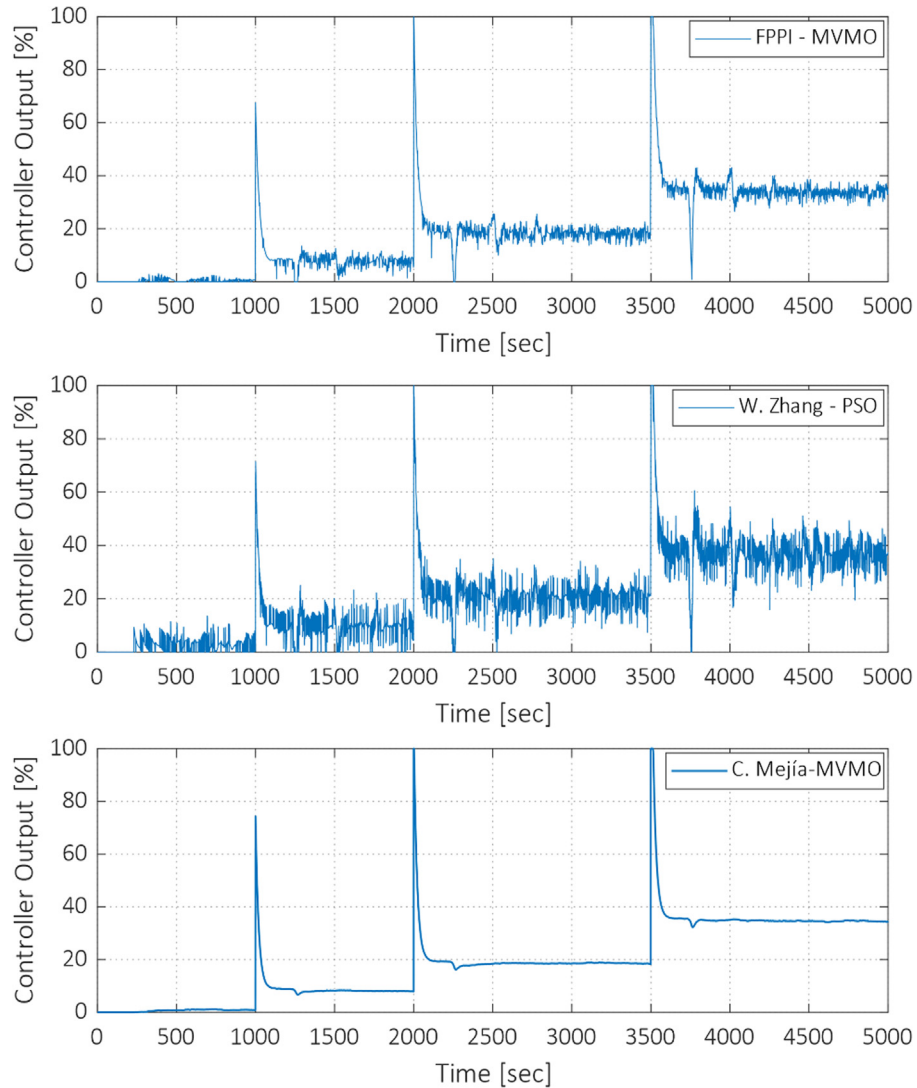


Fig. 23 The control signal for the three control schemes.

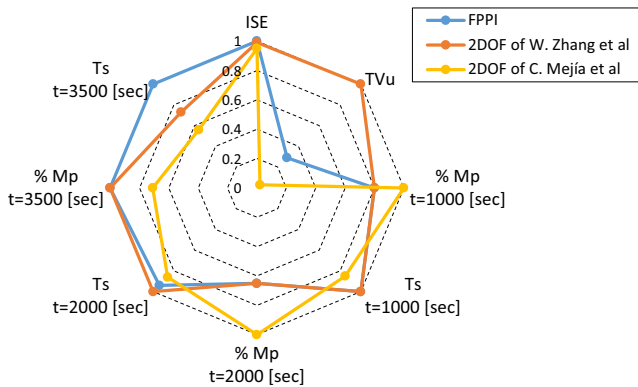


Fig. 24 Performance indices comparison for the three control schemes.

It can be seen that the 2DOF control scheme of Zhang et al. compensates for the disturbances faster than the other two control schemes.

Fig. 26 shows the control actions when disturbances appear in the temperature process. It illustrates that the control schemes adequately compensate for the disturbances by increasing or decreasing the control action. Also, it can be said that the 2DOF control scheme of C. Mejia et al. presents the smoothest control action compared to the other two schemes. However, the FPPI control scheme has less noise in the control signal than the 2DOF scheme of Zhang et al. because it has a filter in its structure.

Summarizing the previous two graphs, despite that the 2DOF control scheme of W. Zhang et al. compensates for the disturbances faster than the other two control schemes, its control effort is the worst from the final element lifetime point of view.

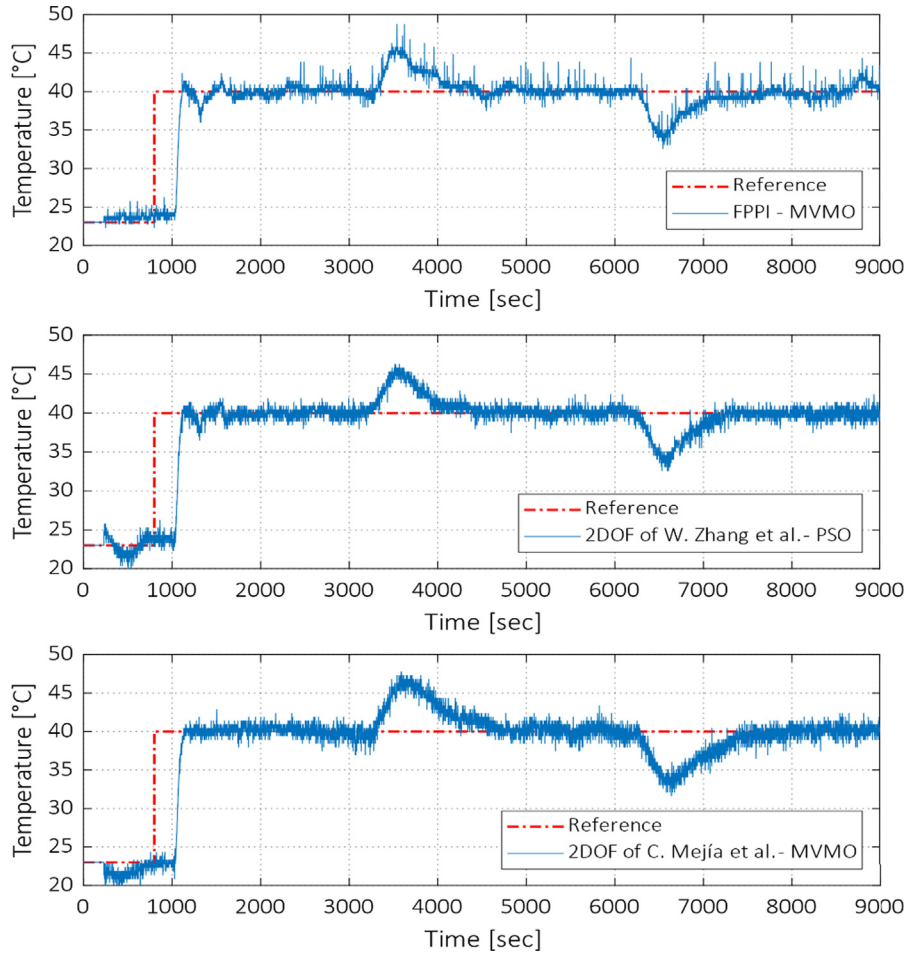


Fig. 25 Output process for the three control schemes when disturbances occur.

In Fig. 27, a radial graph compares the different performance indices obtained when making disturbances in the temperature process to see how the different indices perform. The radial graph of Fig. 27 illustrates that the 2DOF control scheme of C. Mejía et al., tuned by MVMO, performs better than the FPPI schemes tuned by MVMO and the 2DOF scheme of W. Zhang et al. adjusted by PSO since the 2DOF scheme of C. Mejía has the smallest area in the radial graph.

6. Conclusions

This paper emphasized a comparative experimental evaluation of various Smith predictor configurations available in the control literature to control the outlet temperature of a TCLAB. An identification procedure using real-time data of the TCLAB has been carried out to obtain a linear model for tunings the different control approaches. The resulting model is a first-order plus time-delay with a controllability relationship greater than one, which means that the time delay term is dom-

inant concerning its time constants. Validation showed a good agreement between experimental and model-based data.

Three Smith predictor-based control schemes have been studied, implemented, and compared in the TCLAB. Comparison of actual results showed that the modification of the SP scheme proposed by Mejía et al. [16] yielded the best results in step disturbance rejection. Moreover, it was the first time used in experimental evaluation.

The controllers were tuned using three different optimization algorithms to choose the best option for each scheme. The optimization methods used were MVMO, GA, and PSO. It is the first time that MVMO is used to tune the SP and the results showed that MVMO presented a better global performance than the other two methods.

The experimental comparative evaluation of the three control schemes was carried out using the Temperature Control Laboratory (TCLab). They were evaluated under different conditions and performance indices for tracking and disturbances changes. All the performance index results were sum-

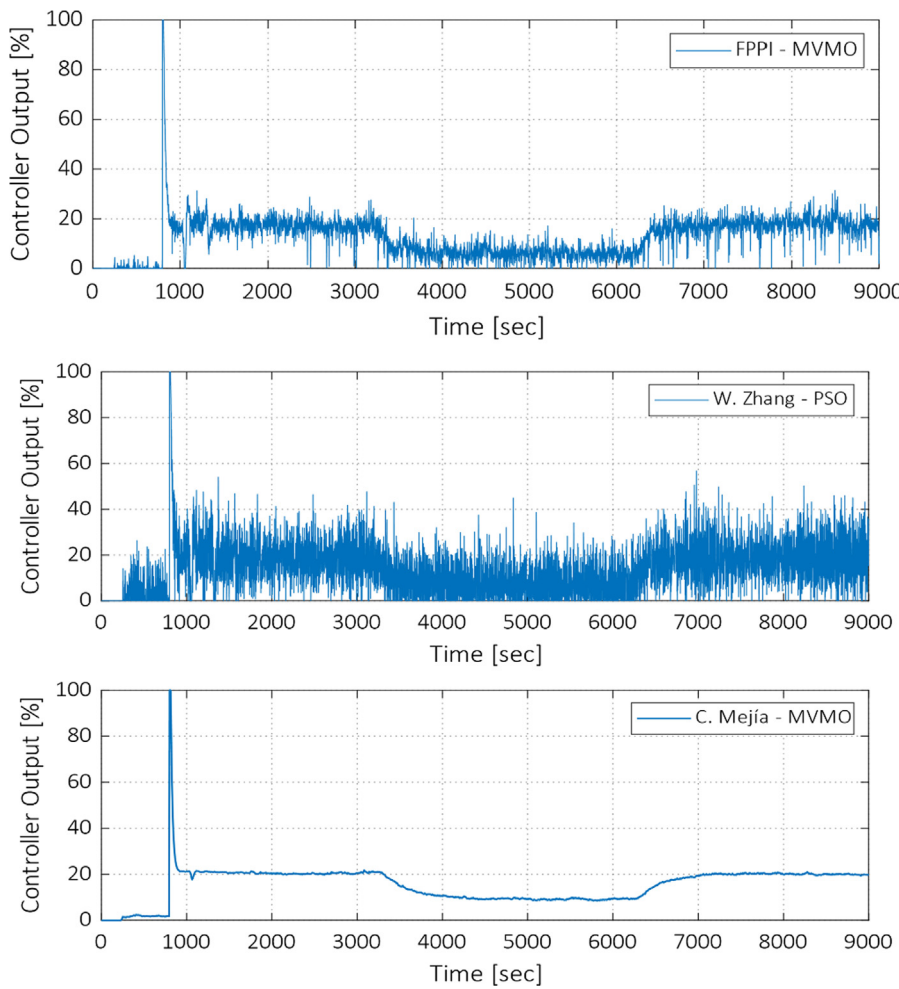


Fig. 26 The control signal for the three control schemes when disturbances occur.

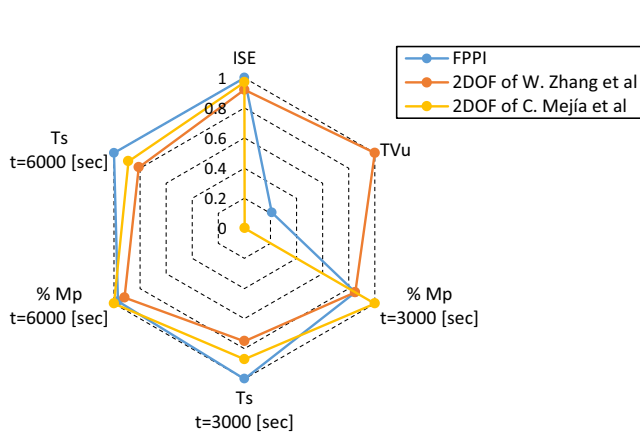


Fig. 27 Performance indices comparison for the three control schemes when disturbances occur.

marized using the radial graphs, and from them, the Mejia et al. approach presented a better overall performance than the other two.

Declaration of Competing Interest

The authors declare that they have no known competing financial interests or personal relationships that could have appeared to influence the work reported in this paper.

References

- [1] M. Jayachandra Babu, N. Sandeep, Effect of nonlinear thermal radiation on non-aligned bio-convective stagnation point flow of a magnetic-nanofluid over a stretching sheet, *Alex. Eng. J.* 55 (3) (2016) 1931–1939.
- [2] E. Baez, Y. Bravo, P. Leica, D. Chávez, O. Camacho, Dynamical sliding mode control for nonlinear systems with variable delay, in: IEEE, 3rd Colombian Conference on Automatic Control (CCAC), 2017, pp. 1–6.
- [3] O. Camacho, H. Leiva, Impulsive semilinear heat equation with delay in control and in state, *Asian J. Control* 22 (3) (2020) 1075–1089.
- [4] O. Camacho, J. Martínez, Procesos con Retardo de Tiempo Dominante. Diseño, Análisis y Comparación de Estrategias de Control. Editorial Académica Española. Saarbrücken, Alemania, 2017.
- [5] R.K. Arora, Optimization: Algorithms and Applications, Chapman and Hall/CRC, 2019.

- [6] I. Erlich, G.K. Venayagamoorthy, N. Worawat, A mean-variance optimization algorithm, IEEE Congress on Evolutionary Computation, Barcelona, Spain, 2010, pp. 1–6.
- [7] E. Fridman, Introduction to time-delay systems: analysis and control, Springer, 2014.
- [8] M. Huba, P. Bistak, D. Vrancic, K. Zakova, Deadtime compensation for the first-order dead-time processes: towards a broader overview, *Mathematics* 9 (13) (2021) 1519.
- [9] H.-P. Huang, C.-L. Chen, Y.-C. Chao, P.-L. Chen, A modified smith predictor with an approximate inverse of dead time, *AICHE J.* 36 (7) (1990) 1025–1031.
- [10] J. Jia, H. Liu, C. Xu, F. Yan, Dynamic effects of time delay on a coupled FitzHugh–Nagumo neural system, *Alex. Eng. J.* 54 (2) (2015) 241–250.
- [11] V. Kachitvichyanukul, Comparison of three evolutionary algorithms: GA, PSO, and DE, *Ind. Eng. Manage. Syst.* 11 (3) (2012) 215–223.
- [12] V.L. Korupu, M. Muthukumarasamy, A comparative study of various Smith predictor configurations for industrial delay processes, *Chem. Prod. Process Model.* (2021).
- [13] R. Sivaramakrishnan, C. Arun, Performance evaluation of bio-inspired optimization algorithms in resolving chromosomal occlusions, in: 2014 International Conference on Control, Instrumentation, Communication and Computational Technologies (ICCICCT), IEEE, 2014, pp. 48–54.
- [14] B. Mahanthesh, B.J. Gireesha, R.S.R. Gorla, Heat and mass transfer effects on the mixed convective flow of chemically reacting nanofluid past a moving/stationary vertical plate, *Alex. Eng. J.* 55 (1) (2016) 569–581.
- [15] T.E. Marlin, Process control, in: Design Processes and Control Systems for Dynamic Performance. Boston, Mass: McGraw-hill; 2015.
- [16] C. Mejía, O. Camacho, D. Chávez, M. Herrera, A modified smith predictor for processes with variable time delay, in: IEEE, 4th Colombian Conference on Automatic Control (CCAC), 2019, pp. 1–6.
- [17] M.J. Moran, H.N. Shapiro, B.R. Munson, D.P. DeWitt, *Introduction to Thermal Systems Engineering: Thermodynamics, Fluid Mechanics, and Heat Transfer*, John Wiley & Sons, 2002.
- [18] J.E. Normey Rico, Predicción para Control. Tesis doctoral. Escuela Superior de Ingenieros, Universidad de Sevilla, 1999.
- [19] J.E. Normey Rico, E.F. Camacho, *Predicción para Control: Una Panorámica del Control de Procesos con Retardo*, RIAI 3 (4) (2006) 5–25.
- [20] J.E. Normey Rico, E.F. Camacho, *Control of Dead-Time Processes*, Springer-Verlag, London Ltd, 2007.
- [21] B.A. Ogunnaike, W.H. Ray, *Process Dynamics, Modeling and Control*, Oxford Univ. Press, New York, 1994.
- [22] P.M. Oliveira, J.D. Hedengren, An APMonitor temperature lab PID control experiment for undergraduate students, in: IEEE, 24th Conference on Emerging Technologies and Factory Automation (ETFA), 2019, pp. 790–797.
- [23] N.S. Özbek, İ. Eker, A fractional fuzzy PI-PD based modified Smith predictor for controlling of FOPDT process, in: IEEE, 5th International Conference on Electronic Devices Systems and Applications (ICEDSA), 2016, pp. 1–4.
- [24] Z.J. Palmor, D.V. Powers, Improved dead-time compensator controllers. Improved deadtime compensator controllers, *AICHE-J* 31 (2) (1985) 215–221.
- [25] J. Park, R.A. Martin, J.D. Kelly, J.D. Hedengren, Benchmark temperature microcontroller for process dynamics and control, *Comput Chem Eng* 135 (2020) 106736, <https://doi.org/10.1016/j.compchemeng.2020.106736>.
- [26] J.A. Rossiter, S.A. Pope, B.L. Jones, J.D. Hedengren, Evaluation and demonstration of take-home laboratory kit, *IFAC-PapersOnLine* 52 (9) (2019) 56–61.
- [27] M. Sen, A review of principles and applications of thermal control, *Ingen. Mecá. Tecnol Desarr* 1 (4) (2004) 115–131.
- [28] C.A. Smith, A.B. Corripio, *Principles and Practice of Automatic Process Control*. New York: J. Wiley; 1997.
- [29] Weidong Zhang, Youxian Sun, Xiaoming Xu, Two degree-of-freedom smith predictor for processes with time delay, *Automática* 34 (10) (1998) 1279–1282.